An In-silico Study of Sex Differences in Carotid Hemodynamic Waveforms

Irene Suriani[1], R Arthur Bouwman[2], Massimo Mischi[1], Kevin D Lau[3]

[1]Eindhoven University of Technology, Eindhoven, The Netherlands
[2]Catharina Hospital, Eindhoven, The Netherlands
[3]Philips Research, Eindhoven, The Netherlands

Abstract

Arterial stiffening, a natural process occurring with age, is a recognized risk factor for cardiovascular disease. Sex differences in vascular aging have been observed, with females experiencing increased aortic stiffness after menopause. Carotid hemodynamic waveforms-derived pressure and flow augmentation indices (pAIx and fAIx) are considered a potential tool for the non-invasive assessment of arterial stiffness. These tend to be higher in females, with a larger age-related increase. Alongside differences in arterial stiffness, other factors such as smaller height have been suggested as contributing factors. This in-silico study employs one-dimensional (1D) hemodynamic modeling to explore the determinants of sex-related differences in carotid augmentation indices. Male and female-representative in-silico carotid waveforms at the 3rd and 6th age decades were generated by parametrizing the models based on a literature survey of cardiovascular sex differences. Realistic sex differences in augmentation indices were reproduced by the models. Furthermore, a sensitivity analysis was performed to compare the effect of individual parameters on both pAIx and fAIx. Our findings reveal a variety of factors strongly influencing these indices, with a significant role played by the relative size of second-generation arteries with respect to the aorta.

1. Introduction

Cardiovascular aging is a natural process causing the progressive deterioration of several heart and vascular properties affecting circulatory function. Among the most concerning phenomena is age-related arterial stiffening, which is a known risk factor for cardiovascular disease [1]. Research has shown that vascular aging progresses differently in males and females, with aortic stiffness being lower in females during reproductive age, while sharply increasing to values higher than males' around menopause, as attributed to hormonal effects [2]. Carotid hemodynamic waveforms, which can be measured non-invasively via Doppler ultrasound and arterial tonometry, offer valuable insights into cardiovascular age and health. Specifically, carotid pressure and flow augmentation indices (pAIx and fAIx, respectively), which quantify the influence of wave reflection on systolic flow and pressure, are considered markers of arterial stiffening [3].

These indices have been observed to be higher in females, with pAIx reportedly showing a steeper age-related increase in females [4], [5]. While sex-related differences in arterial stiffness at an older age are assumed to contribute to this phenomenon, other aspects such as smaller height and higher aortic tapering in females have been proposed as additional influential factors [4], and may explain the sex differences in AIx at a younger age.

In this study, one-dimensional (1D) hemodynamic modeling was employed to investigate the determinants of sex-related differences in carotid augmentation indices. By utilizing average parameter values from literature data for males and females (including heart rate, stroke volume, aortic tapering, arterial lengths, diameters, and stiffnesses) virtual subjects representing young adults (3rd age decade) and elder/post-menopausal (6th age decade) individuals of both sexes were generated and the resulting carotid in-silico pressure and flow waveforms were compared.

Furthermore, a local sensitivity analysis was performed by systematically adjusting individual parameters from their baseline value to their ± standard deviations (sd), observing the resulting changes in carotid waveform morphology, and quantifying their elementary effect on both augmentation indices by computing relative sensitivity indices.

This investigation aims to provide a clearer understanding of the mechanisms behind sex-related differences in carotid augmentation indices.

2. Methods

2.1. One-dimensional (1D) hemodynamic modeling

In 1D modeling, a system of constitutive equations describing fluid dynamics through compliant vessels is solved throughout a defined arterial network, allowing to obtain hemodynamic waveforms, including pressure and flow, at any arterial cross-section of interest [6]. Arteries are assigned geometrical and material properties (length, diameter, taper, stiffness). At the inlet of the model, an aortic inflow waveform is prescribed, and at the terminal

branches, RCR Windkessel elements are connected, to account for peripheral resistance, compliance, and reflections [6]. In this work, the 1D formulation described in [7], which employs a purely elastic tube law, was adopted, and equations were solved by means of a Discontinuous Galerkin finite element scheme, with time integration via the explicit second-order Adam-Bashforth method. Time stepping was performed at 0.5 ms, and 15 seconds were run to ensure convergence of the simulation. This was implemented using a modified version of the NEKTAR++ Pulse Wave Solver [8]. A validated 55-branch arterial network topology [6], as shown in [7], was adopted.

2.2. Sex-specific parametrization

For the male virtual subject in the 3rd age decade, the baseline parameter set detailed in [7] was utilized, comprising of dimensions and material properties for each of the 55 arteries included in the model, and RCR Windkessel parameters at the terminal branches. At the inlet of the model, we prescribed an inflow waveform scaled to a heart rate (HR) of 65 bpm, and a cardiac output (CO) of 6.17 L/min. Arterial stiffness was set via the local wave speed parameter c for each artery. All parameters were scaled as described in a previous study [7] to obtain the male virtual subject in the 6th age decade. To obtain the age-matched female subjects, the parameter variations listed in Table 1 were applied with respect to the corresponding male value, following a literature survey.

Table 1. Variations applied to each model parameter of the male virtual subjects at the two age decades to obtain age-matched females.

Model parameter	3rd age decade	6th age decade	Ref.
Aortic length (L_{ao})	-7%	-7%	Weir-McCall 2018
Aortic taper (t_{ao})	+16%	+16%	London 1995
Aortic c (c_{ao})	-10%	+10%	Nethononda 2015
Carotid c (c_{car})	0%	+5%	Uejima 2005
Muscular* c (c_{musc})	0%	0%	Ahlgren 2011
Aortic diameter (d_{ao})	-10%	-7%	Agmon 2003
Carotid diameter (d_{car})	-25%	-10%	Sass 1998, Lefferts 2020, Hansen 1995
Muscular* diameters (d_m)	-25%	-10%	Sass 1998, Joannides 2001, Sandgren 1999, Van der Heijden-Spek 2000
Heart rate (HR)	+7%	+7%	Segers 2007, St-Pierre 2020
Cardiac output (CO)	-25%	-25%	Segers 2007, St-Pierre 2020

*All arteries except for the aorta and common carotid.

2.3. Calculation of augmentation indices

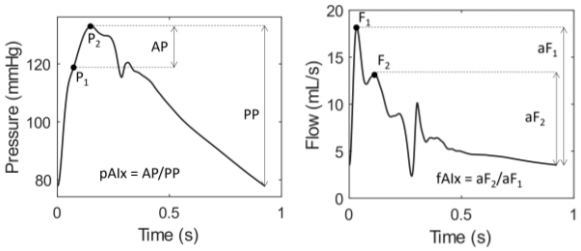

Figure 1: Calculation of pAIx and fAIx from fiducial points. AP augmentation pressure, PP pulse pressure, aF_1 and aF_2 amplitude of the first and secondary systolic peaks, respectively.

Augmentation indices were calculated via the formulas illustrated in Fig. 1. The necessary fiducial points were detected on the waveforms via automated algorithms. In particular, P_1 was detected as the second local maximum on the 2nd derivative of pressure [9], and F_2 as the second gradient sign change after F_1 [10].

2.4. Analysis of the sensitivity of augmentation indices to model parameters

To discern the influence of each parameter on the augmentation indices, a local sensitivity analysis was performed. One parameter at a time was varied from baseline value to ±sd, while the rest was kept at baseline value. The relative sensitivity σ_{ik} of augmentation index AIx_k = {pAIx, fAIx} with respect to variation v of the parameter p_i (i ∈ [1:10]) was calculated using the central finite difference method approximation, as:

$$\sigma_{ik} = \frac{AIx_k\left(p_i^{+sd},\ p_j\right) - AIx_k(p_i^{-sd}, p_j)}{AIx_k(p_i^0, p_j)} \cdot \left(\frac{1}{v}\right) \qquad (1)$$

with $p_i^{0,\mp sd}$ being one of the parameters listed in Table 1 at baseline value or varied by ±sd, p_j ($j \neq i$) all other parameters kept at baseline value, and $v = \frac{p_i^{+sd} - p_i^{-sd}}{p_i^0}$ [11].

3. Results

3.1. Simulated sex-specific carotid hemodynamic waveforms

Fig. 2 and 3 show the simulated carotid hemodynamic waveforms of the young adult and post-menopausal age models, respectively, with the corresponding pAIx and fAIx values. At both ages, augmentation indices are higher in the female models.

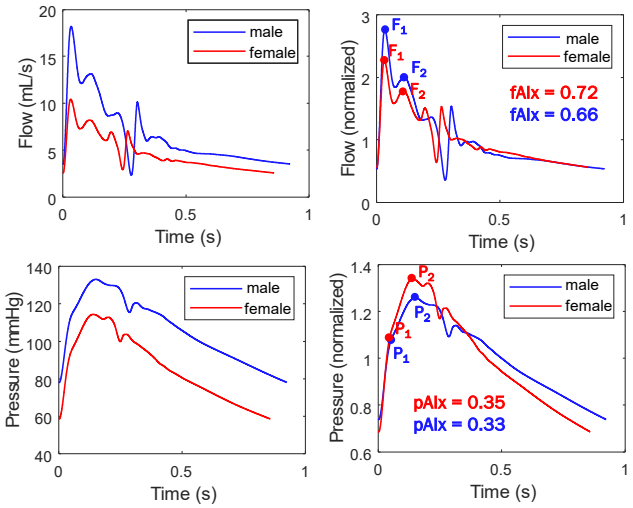

Figure 2: Carotid pressure and flow waveforms of the male and female young adult models (3rd age decade). On the right-most plots, waveforms are normalized by their mean for better morphological comparison. Fiducial points AIx values are reported.

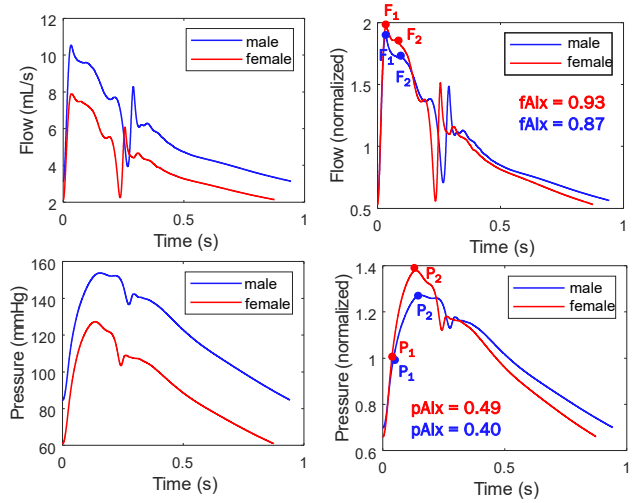

Figure 3: Same as Fig.2, for post-menopausal/older adult models (6th age decade).

3.2. Impact of individual parameters on the augmentation indices

Figure 4 shows the sensitivity of pAIx and fAIx to each parameter considered (see Table 1 for acronyms). A major impact was observed for aortic stiffness (see also Figure 5), relative size of different arterial groups, and aortic length. Notably, pAIx was also sensitive to CO, whereas its effect on fAIx was small.

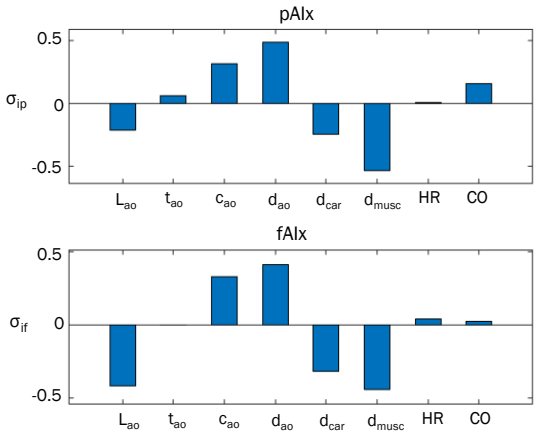

Figure 4: Relative sensitivity of pAIx and fAIx (σ_{ip} and σ_{if} respectively) to each of the model parameters (x-axis).

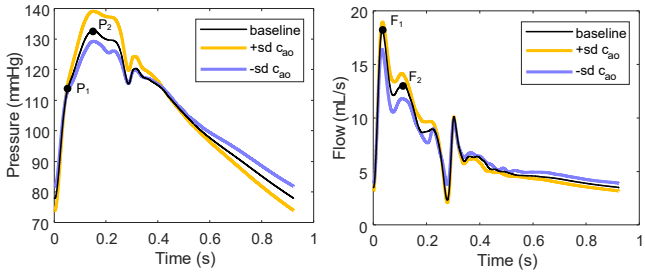

Figure 5: Effect of varying c_{ao} by ±sd on the carotid flow and pressure waveforms.

4. Discussion

The simulated carotid waveforms (Section 3.1) show realistic morphology for the different sexes and ages. As shown in Figure 2, the female model exhibits lower mean flow (top left-most plot), lower flow pulsatility, and higher flow augmentation (top right-most plot) compared to the male, as reported in-vivo [12]. Mean pressure is also lower (bottom left-most plot) and pressure augmentation higher in the female model (bottom right-most plot) [4], [5]. A lower mean pressure is explained by the fact that CO was lower in female models, whereas systemic vascular resistance was kept unchanged as no significant differences between the sexes has been reported [13], [14]. Similar differences are observed for the older/post-menopausal models (Figure 3), and pAIx difference is exacerbated compared to the younger models, as reported in-vivo (see Figure 6) [4], [5].

Figure 4 shows the impact of various model parameters on both pAIx and fAIx, indicating that the disparities observed between males and females may be attributed to a combination of contributing factors. Firstly, as expected, an increase in c_{ao} results in an increase in both pAIx and fAIx (see also Figure 5).

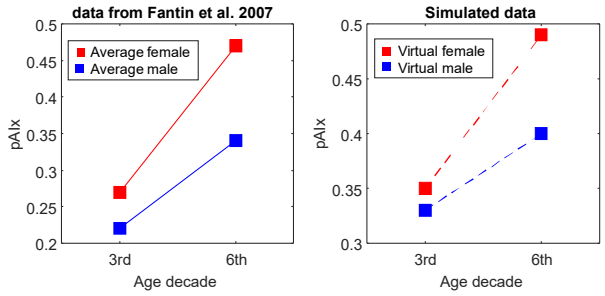

Figure 6: pAIx values in the virtual males and females at the two age decades, compared to corresponding average values measured in-vivo in a population.

While this effect may partly elucidate the elevated AIx in post-menopausal females, who typically exhibit higher c_{ao} compared to age-matched males, it does not account for the observed difference in younger females, where c_{ao} is actually lower than males [2], and other factors must therefore play a dominant role.

One of these appears to be the average height difference between males and females. Notably, an increase in L_{ao} is seen to result in a substantial decrease in both AIx. Moreover, a major effect is observed upon individually varying the diameter of different arterial groups. This phenomenon is due to alterations in the impedance mismatch between the aorta and second-generation vessels, which dictates the magnitude of wave reflections responsible for systolic augmentation [15]. In particular, in younger females, who have proportionally smaller muscular arteries in relation to the aorta, this may be the primary explanation for the higher AIx values despite exhibiting a lower c_{ao} than age-matched males [2].

Finally, pAIx was observed to be sensitive to CO variations, aligning with existing literature indicating a positive correlation between pAIx and ejection duration [16], which is linked to CO [17]. In contrast, fAIx exhibited little sensitivity to this parameter.

These findings have noteworthy implications for the clinical interpretation of carotid AIx. While AIx are typically considered markers of arterial stiffness, our study highlights their susceptibility to various cardiovascular properties. These results suggest that adjustment of AIx by height is advisable. Moreover, their relation to arterial size should be kept in mind, as this appears to be a primary determinant of their value. Finally, fAIx appears to be more robust than pAIx to variations in CO.

5. Conclusions

In this study, sex-specific models were generated for two different age groups, enabling the replication of physiological differences in carotid waveform morphology and AIx. Several factors contributing to sex-related differences in pAIx and fAIx were revealed through a local sensitivity analysis of the baseline model, including differences in aortic stiffness, aortic length, and relative size of second-generation arteries with respect to the aorta.

References

[1] C. Vlachopoulos et al., "Prediction of cardiovascular events and all-cause mortality with arterial stiffness: a systematic review and meta-analysis," *J. Am. Coll. Cardiol.*, vol. 55, no. 13, pp. 1318–1327, Mar. 2010.

[2] R. M. Nethononda et al., "Gender specific patterns of age-related decline in aortic stiffness: A cardiovascular magnetic resonance study including normal ranges," *J. Cardiovasc. Magn. Reson.*, vol. 17, no. 1, pp. 1–9, 2015.

[3] J. Hashimoto et al., "Carotid Flow Augmentation, Arterial Aging, and Cerebral White Matter Hyperintensities: Comparison with Pressure Augmentation," *Arterioscler. Thromb. Vasc. Biol.*, vol. 38, no. 12, pp. 2843–2853, 2018.

[4] C. S. Hayward et al., "Gender-Related Differences in the Central Arterial Pressure Waveform," *J. Am. Coll. Cardiol.*, vol. 30, no. 7, pp. 1863–1871, 1997.

[5] F. Fantin et al., "Is augmentation index a good measure of vascular stiffness in the elderly?," *Age Ageing*, vol. 36, no. 1, pp. 43–48, 2007.

[6] J. Alastruey et al., "Arterial pulse wave haemodynamics," in *11th International Conference on Pressure Surges*, 2012.

[7] I. Suriani et al., "An in-silico study of the effects of cardiovascular aging on carotid flow waveforms and indices in a virtual population," *Manuscr. under Rev. AJP-Heart*.

[8] S. Sherwin and M. Kirby, "Nektar++ Spectral/hp Element Framework." https://www.nektar.info/

[9] P. Segers et al., "Assessment of pressure wave reflection: Getting the timing right!," *Physiol. Meas.*, vol. 28, no. 9, pp. 1045–1056, 2007.

[10] M. N. Gwilliam et al., "MR derived volumetric flow rate waveforms at locations within the common carotid, internal carotid, and basilar arteries," *J. Cereb. Blood Flow Metab.*, vol. 29, no. 12, pp. 1975–1982, 2009.

[11] C. A. D. Leguy et al., "Global sensitivity analysis of a wave propagation model for arm arteries," *Med. Eng. Phys.*, vol. 33, no. 8, pp. 1008–1016, 2011.

[12] Y. Hoi et al., "Characterization of volumetric flow rate waveforms at the carotid bifurcations of older adults," *Physiol. Meas.*, vol. 31, no. 3, pp. 291–302, 2011.

[13] P. Segers et al., "Wave Reflection in Healthy Middle-Aged Men and Women," pp. 1248–1255, 2007.

[14] R. T. Sless et al., "Sex differences in pulmonary and systemic vascular function at rest and during exercise in healthy middle-aged adults," *J. Hum. Hypertens.*, pp. 1–16, 2023.

[15] J. P. Mynard et al., "Measurement, Analysis and Interpretation of Pressure/Flow Waves in Blood Vessels," *Front. Physiol.*, vol. 11, no. August, pp. 1–26, 2020.

[16] J. E. Sharman et al., "Augmentation index, left ventricular contractility, and wave reflection," *Hypertension*, vol. 54, no. 5, pp. 1099–1105, 2009.

[17] A. M. Weissler et al., "Relationships between left ventricular ejection time, stroke volume, and heart rate in normal individuals and patients with cardiovascular disease," *Am. Heart J.*, vol. 62, no. 3, pp. 149–159, 1961.

Address for correspondence: i.suriani@tue.nl